AD-A112 842 ADVANCED RESEARCH AND APPLICATIONS CORP SUNNYVALE CA F/G 20/12
METAL-SEMICONDUCTOR REACTION PHENOMENA AND MICROSTRUCTURAL INVE--ETC(U)
JAN 82 T J MAGEE, C LEUNG, R D ORMOND DAAG29-79-C-0014
UNCLASSIFIED ARACOR-FR-82-37-1 ARO-15999.6-MS NL

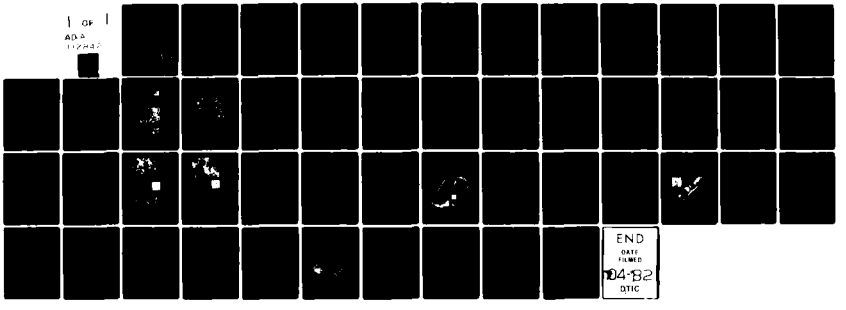

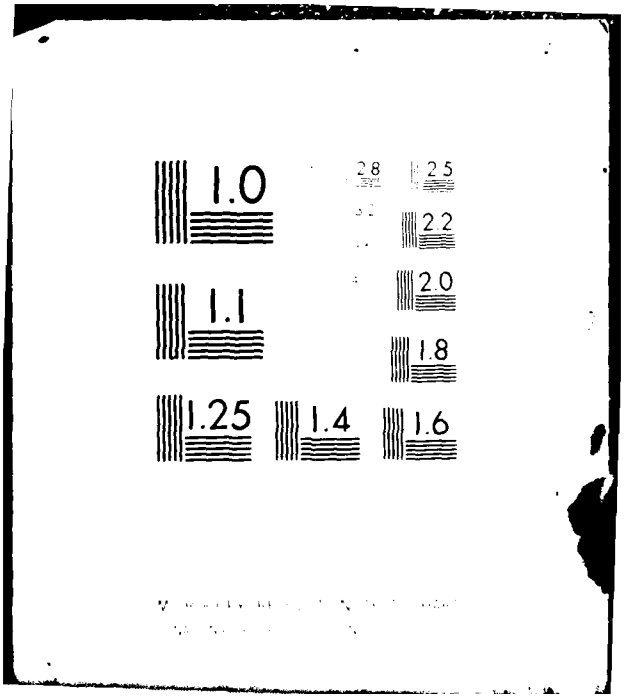
1.0
2.8
2.5
2.2
1.1
2.0
1.8
1.25
1.4
1.6

ARO 15999.6-MS

(12)

AD A112 ...

METAL-SEMICONDUCTOR REACTION PHENOMENA AND MICROSTRUCTURAL INVESTIGATIONS OF LASER INDUCED REGROWTH OF SILICON ON INSULATORS

FINAL REPORT

JANUARY 1982

PREPARED FOR:

U.S. ARMY RESEARCH OFFICE
CONTRACT NO. DAAG29-79-C-0014

APPROVED FOR PUBLIC RELEASE
DISTRIBUTION UNLIMITED

ADVANCED RESEARCH AND APPLICATIONS CORPORATION

82 03 29 004

UNCLASSIFIED

SECURITY CLASSIFICATION OF THIS PAGE (When Data Entered)

REPORT DOCUMENTATION PAGE		READ INSTRUCTIONS BEFORE COMPLETING FORM
1. REPORT NUMBER FR-82-37-1	2. GOVT ACCESSION NO. AD-A112 142	3. RECIPIENT'S CATALOG NUMBER
4. TITLE (and Subtitle) Metal-Semiconductor Reaction Phenomena and Microstructural Investigations of Laser-Induced Regrowth of Silicon on Insulators		5. TYPE OF REPORT & PERIOD COVERED Final Report Jan. 1979 to Jan. 1982 6. PERFORMING ORG. REPORT NUMBER
7. AUTHOR(s) T.J.Magee ,C.Leung, R.D.Ormond and R.A. Armistead		8. CONTRACT OR GRANT NUMBER(s) DAAG29-C-0014 79
9. PERFORMING ORGANIZATION NAME AND ADDRESS Advanced Research and Applications Corporation 1223 E. Arques Avenue Sunnyvale, CA 94086		10. PROGRAM ELEMENT, PROJECT, TASK AREA & WORK UNIT NUMBERS
11. CONTROLLING OFFICE NAME AND ADDRESS U.S. Army Research Office P.O.Box 12111 Research Triangle Park, NC 27709		12. REPORT DATE January, 1982 13. NUMBER OF PAGES
14. MONITORING AGENCY NAME & ADDRESS(if different from Controlling Office)		15. SECURITY CLASS. (of this report) UNCLASSIFIED 15a. DECLASSIFICATION/DOWNGRADING SCHEDULE NA

16. DISTRIBUTION STATEMENT (of this Report)

Approved for public release; distribution unlimited.

17. DISTRIBUTION STATEMENT (of the abstract entered in Block 20, if different from Report)

NA

18. SUPPLEMENTARY NOTES

The findings in this report are not to be construed as an official Department of the Army position, unless so designated by other authorized documents.

19. KEY WORDS (Continue on reverse side if necessary and identify by block number)

Thin films	Silicon-on-sapphire	Stacking faults
Metal-semiconductor reactions	Microstructural defects	Spreading epitaxy
Transmission electron microscopy	Rutherford backscattering	Silicon
Liquid phase epitaxy	Laser annealing	Gallium Arsenide
Solid phase epitaxy	Electrical contacts	Diffusion

20. ABSTRACT (Continue on reverse side if necessary and identify by block number)

Solid phase regrowth of Silicon-on-sapphire has been investigated in the Si (amorphous)/Al(poly) Al_2O_3 (crystal) system. Using transmission electron microscopy, scanning electron microscopy, Auger electron spectroscopy and Hall effect measurements, it has been shown that Si is transported through an Al film at 550°C to produce p-type Si films on the sapphire substrate. The growth process has been shown to initiated at Si nucleation sites on the substrate. These sites expand by mass accretion forming island structures

DD FORM 1 JAN 73 1473 EDITION OF 1 NOV 65 IS OBSOLETE UNCLASSIFIED

SECURITY CLASSIFICATION OF THIS PAGE (When Data Entered)

that coalesce to yield continuous large grained polycrystalline Si films on the sapphire surface.

The defect structure in CVD Si layers on sapphire were investigated before and after scanning laser annealing. Prior to laser annealing, the films were characterized by the presence of stacking faults, twinning zones and dislocation lines producing large regions of high disorder. Subsequent to laser annealing under conditions to produce total melting of the Si layers it was shown that liquid phase epitaxial regrowth occured resulting in regions of defect-free Si and a total absence of twinning regions. Correlated Rutherford backscattering, channeling and transmission electron microscopic analyses showed a dramatic improvement in crystalline perfection relative to the results obtained from films grown by any other technique on sapphire substrates.

Single-crystal Si sheets (0.2 μm in thickness) of (100) orientation and of maximum dimensions, 100 x 10,000 μm, have been recrystallized by cw laser annealing of polycrystalline Si films deposited over parallel 3- μm-wide SiO_2 bars adjacent to 3- μm Si (100) substrate openings. The recrystallized films are free of cracks, mosaic structure, stacking faults, or excessive mass flow at the oxide edges. In a correlated series of experiments we have shown that the Si can be recrystallized over the SiO_2 with only limited or relaxed requirements for verical seeding from the substrate window.

In separate collaborative experiments with Stanford University, it was also shown that scanning cw laser irradiation could be used to produced diffusion and activation of Sn from a spin-on SnO_2/SiO_2 source. The formation of a Sn_3As_2 alloy ahs been shown to be related to the observed n^+ activity.

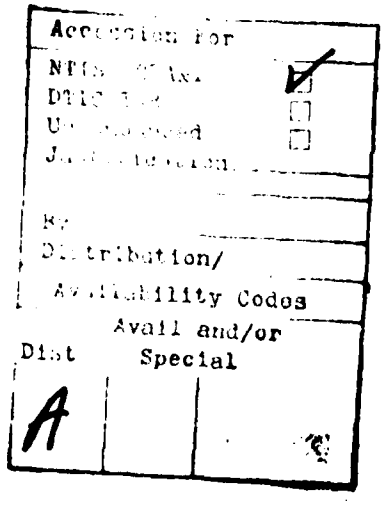

CONTENTS

FIGURES

TABLES

1.0 INTRODUCTION

Reactions between metal films and single or polycrystalline silicon substrates have received considerable attention over the past decades because of the relevancy to integrated circuit fabrication and design. The aluminum-silicon (Al/Si) system has been widely investigated in relation to its use in contact structures, as a diffusion source and in silicon-gate MOS technology.

In an early phase of this program, it was shown that interactions between a polycrystalline Al film and single-crystal Si were controlled, in part, by grain boundary kinetics and the presence of microstructural defects within individual Al grains. Interdiffusion between the Al and Si was initiated at Al grain boundary sites and within defective Al grains producing Si-saturated Al films and localized Al-doped regions within the Si substrate. Upon cooling, lateral motion of Si to grain boundaries occurred, accompanied by a solid-phase regrowth of silicon hillocks on the single-crystal substrate.

Subsequent experiments conducted on the Al(poly)/Si (poly) /SiO_2/Si (crystal) system showed that after heating at 500°C, Si was transported through the Al film to form a continuous Si film at the surface. Growth was initiated at grain boundaries of the Al film and individual growth islands expanded by lateral accretion, yielding a coalesced continuous poly-Si film at the surface.

The data obtained in these experiments suggested that the solid-phase regrowth process was controlled by the relative grain sizes of the silicon and aluminum (g_{Si}/g_{Al}) and

relative thickness (t_{Si}/t_{Al}). Research in the first phase of the current program tended to verify these assumptions, confirming that as $g_{Si}/g_{Al} \rightarrow \infty$(for $t_{Si}/t_{Al} \rightarrow 1$,), solid-phase interchange of layer positions was relatively inhibited.

To extend these results, we conducted a series of experiments on regrowth of Si on sapphire in the Si(amorphous)/Al(poly)/Al_2O_3(crystal) system. The primary objective was to determine if the solid-phase regrowth process could be correlated with a classical island growth/coalescence model within a known system, where island coalescence is the dominant mechanism in epitaxial growth.

These experiments demonstrated that solid-phase regrowth of Si on sapphire can be obtained using Al as the transport medium. The results showed that the Si is transported through the Al film to form nucleation sites on the sapphire substrate. These sites expand laterally by mass accretion and coalescence to form islands continuous with the underlying substrate. During the final growth sequence, the coalescence of larger island structures is characterized by the presence of twinning zones and defects at the juncture region. Direct observation by TEM/SEM at various stages of annealing confirm that the (structural) regrowth sequence is similar to that observed during conventional growth of Si on sapphire. However, one problem with standard SOS structures is the relatively-high density of twins, stacking faults and dislocation lines in the epitaxial silicon. The regrown silicon layers prepared in these experiments exhibited comparable defect densities and distribution of defects within the Si film.

For electronic device fabrication, it would be very valuable to develop techniques for the growth of epitaxial

silicon on sapphire (or another suitable dielectric substrate) with a low defect concentration. The potential importance of SOS structures is suggested by the fact that a number of organizations proposed the use of SOS structures to satisfy the technical requirements of the current DoD-funded Very-High-Speed Integrated Circuits (VHSIC) Program.

However, in spite of over two decades of research on the growth and control of silicon thin films grown epitaxially on single-crystal sapphire (Al_2O_3), difficult problems remain. Of particular concern is the high level of defects present within the epitaxial Si layer, both at the interface and within the bulk of the film. These defect concentrations influence metal-semiconductor reactions in the contact and interconnection regions and prove to be a severe restrictive factor on the fabrication of devices. The measurable reduction in electron mobility in the presence of these defect strucutures places limits on the speed or switching capability of SOS-based devices.

Recently, a number of investigators have suggested that the quality of silicon layers on sapphire (or, perhaps, some other suitable dielectric substrate) can be improved by pulsed laser irradiation to induce regrowth of the deposited layers by a liquid-phase epitaxial mechanism. Preliminary experiments have also shown that scanning CW argon laser annealing can also produce regrowth of the deposited layers, with an apparent reduction in defect density. In all cases, there have been no detailed investigations of the recrystallization of the Si layers on the microstructural perfection of reordered layers after laser annealing.

Thus, we initiated experiments in collaboration with J. Golecki of Rockwell Labs toward a detailed study of microstructural defects within both control and laser-annealed SOS structures in both the solid-phase regrowth (SPEG) and liquid-phase regrowth (LPE) modes. Correlated data from transmission electron microscopy/diffraction (TEM/TED), scanning electron microscopy (SEM), Auger electron spectroscopy (AES), secondary ion mass spectrometry (SIMS), Rutherford back scattering (RBS), and Hall effect measurements were obtained to provide a consistent description of the regrowth mechanisms and to assess the potential of laser-annealed SOS for device applications.

The recrystallization of amorphous Si thin films over amorphous substrates (SOI) has also been an area of considerable interest and induced melt/recrystallization has been induced by pulsed laser irradiation, scanning laser exposure, strip heater annealing or long-term thermal annealing. Seeded recrystallization, where the melt front initiates from a single crystal region over an amorphous zone, has offered some promise, although detailed experiments have in the past been lacking. Of particular importance has been the absence of carefully controlled experiments defining the parameters influencing growth and/or recrystallization. In this research program, we continued our investigation of "spreading" or bridging epitaxy to delineate factors influencing the initiation of such recrystallization.

In additional experiments, we conducted experiments with Stanford University in support of another ARO-funded program (DAAG-29-78-G-0119) on CW-laser-assisted diffusion and activation of Sn in GaAs from a SnO_2/SiO_2 source. These experiments had a direct relationship to our study of metal-semiconductor reactions and gave us the opportunity to investigate another

metal-semiconductor system. In this report, we will provide a brief description of experiments conducted in each of these areas.

2.0 SOLID-PHASE REGROWTH OF SILICON-ON-SAPPHIRE IN THE $Si/Al/Al_2O_3$ SYSTEM

Solid-phase reactions between Si and Al films and epitaxial regrowth of silicon on single crystal substrates using Al as the transport medium have been reported by a number of investigators.[1-11] In each case, studies reported to date have been concerned primarily with the regrowth kinetics of Si on single crystal Si or amorphous SiO_2 layers. To our knowledge, there have been no published reports on microstructural investigations of solid-phase regrowth of Si on sapphire in the $Si/Al/Al_2O_3$ system. In this section, we present the results of detailed transmission electron microscope/scanning electron micrscope (TEM/SEM) investigations of the transport and regrowth of Si (amorphous) through an evaporated polycrystalline Al film on single-crystal sapphire.

2.1. Preparation of Test Structures

In these experiments, sapphire substrates of $(11\bar{2}0)$ orientation ($\pm 1^{\circ}$) were used. Subsequent to degreasing and cleaning, samples were placed immediately in an oil-free vacuum system, maintained at an initial vacuum level of $\simeq 10^{-7}$ Torr. Aluminum films of 5000 Å thickness were e-beam evaporated at room temperature onto the sapphire wafers. After deposition of the Al layer, the wafer was heated to 300°C or 1 hour in the vacuum system and then allowed to cool for a period of 5 hours. Silicon thin-film layers of $\simeq$5000 Å thickness were next deposited by e-beam evaporation on the Al films and the samples subsequently removed from the vacuum system. Annealing was done in a flowing N_2 environment at 550°C for periods of 1 to 20 hours. After

deposition or annealing, samples were profiled using Auger electron spectroscopy (AES) analyses at an initial vacuum of less than 10^{-10} Torr in a system equipped with dual Ar-ion sputtering guns to provide rapid removal and crater uniformity.

To examine the microstructure of as-deposited Al films, we removed the amorphous Si layer by etching in a dilute HF acid solution, leaving the Al layer intact on the Al_2O_3 substrate. Annealed samples were etched in a warm phosphoric acid solution to remove Al and Si-Al intermixing zones, while retaining Si regrowth structures on the substrate.

Samples were then mounted with wax on a metallic holder and mechnaically ground at the back from an initial thickness of 400 μm to a final thickness of $\simeq$ 20 μm. Specimens were subsequently placed in a Commonwealth Scientific Ar-ion milling unit operated at 8 KV with a 100 A beam current, producing a removal rate of 1 μm/hr. After completing the ion milling step, a thin carbon layer ($\simeq$ 200 Å) was vacuum evaporated on the front surfaces of samples to reduce charging effects in the electron microscope.

2.2 Analysis of Test Structures

After removal of the amorphous Si film, TEM analysis showed that the underlying as-deposited Al film was a fine-grained polycrystalline structure consisting of grains of random orientation and average grain size $\simeq$ 1000 Å. AES analysis of as-deposited Si/Al films on the Al_2O_3 substrate indicated discrete Si and Al film structuress with a thin oxide layer interposed between the two films.

In Fig. 1, we show representative scanning electron micrographs obtained at the sapphire surface after annealing at 550°C for variable periods and removing Al and Al-Si mixture regions by immersion in a phosphoric acid solution. In Fig. 1a, we observe a test structure after annealing for 5 hours which shows a large number of irregular growth nuclei positioned on the sapphire substrate; these were shown by energy-dispersive x-ray analysis to be composed of Si. The particles ranged in size from 1000 Å to 5000 Å and were randomly distributed on the substrate surface. Of particular interest in Fig. 1a, however, is the observed coalescence of nuclei to form growth islands that are laterally separated, but continuous with the underlying substrate.

After 15 hours of annealing, additional growth and lateral expansion of the island structures occured, resulting in a semi-continuous Si-film structure with voids or irregular cavities separating larger regrowth islands (Fig. 1b).

Annealing for 20 hours results in the filling of the voids and the formation of a laterally-continuous film structure of $\simeq$ 5000 Å thickness. Correlated AES profiles confirmed that the Si and Al had interchanged positions after 20 hours of annealing, but that residual Al was present within the regrown Si layer. Additional annealing did not appear to reduce the amount of residual Al within the layer, suggesting that the Al was present in the form of precipitates in the Si film.

To obtain additional information on the nature and crystalline perfection of the low-temperature solid-phase regrowth structures, samples were prepared for TEM analysis. In Fig. 2, we show a representative bright-field transmission

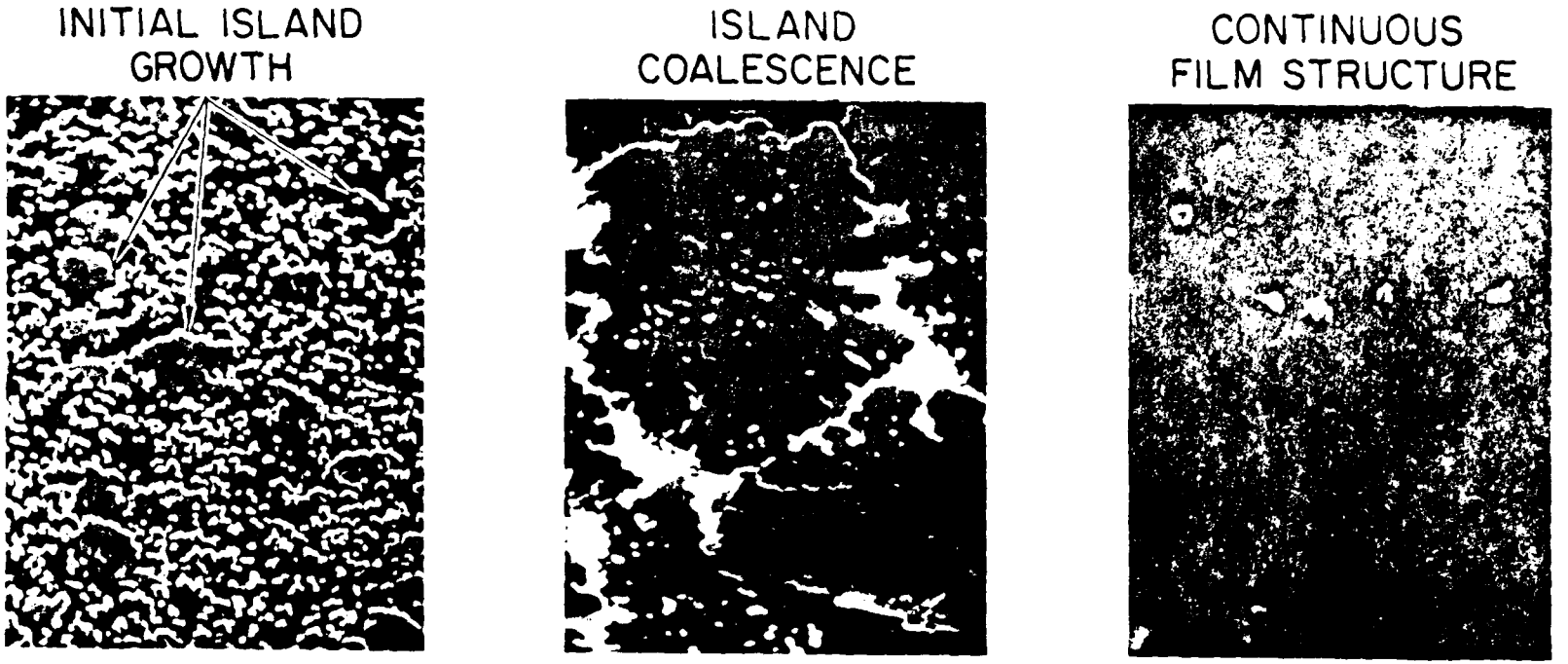

FIG. 1. SCANNING ELECTRON MICROGRAPHS AT SAPPHIRE SURFACE AFTER ANNEALING (550^{o}C) AND IMMERSION IN PHOSPHORIC ACID SOLUTION.

FIG. 2. TRANSMISSION ELECTRON MICROGRAPH OF REGROWN SILICON LAYER ON SAPPHIRE.

electron micrograph of the regrown Si film on sapphire (550°, 20 hours). A number of stacking faults and twinning zones can be observed throughout the film. From a number of micrographs, we detected individual single-crystal growth islands of $\simeq 20\,\mu m$ average size, with defects present at the lateral boundaries of the regrowth structures. These defects are presently thought to arise during the final phases of island coalescence at the juncture between individual growth sites. In all cases, we detected continuous large-grained polycrystalline Si film structures with no evidence of residual Al islands or Al-Si intermixing regions. Selected area electron diffraction revealed the presence of large islands of varying orientation and twinning zones within individual growth sites.

2.3 Measurement of Electrical Characterisitcs

To further investigate the quality of the Si film, we prepared samples for Hall effect measurements in a Van der Pauw configuration to obtain information on the electrical characteristics of the regrown Si layer in comparison to data obtained on Si films grown by solid phase epitaxy on single-crystal silicon. Table 1 lists the data obtained in these experiments and, for reference, includes data reported by Majni and Ottaviani[10-11] on layers regrown on (100) Si. It is of interest to note that the sheet resistivities of the p-type layers are comparable, but that the mobilities differ by a factor of two. The reduction in mobility can be attributed to the presence of defects within the regrown layer on sapphire formed during the transitional growth sequence. In both cases, the data indicate the presence of Al within the Si films, as confirmed by $^4He^+$ backscattering measurements in the experiments of Majni and Ottaviani and by AES profiling in the present study. The measured hole concentration of

3.3×10^{18} cm^{-3} is in agreement with the reported solid solubility of Al[12] at the temperature used in these experiments.

2.4 Discussion

From the data obtained, we can conclude that solid phase regrowth of Si on sapphire can be obtained using Al as the transport medium. The results show that the Si is transported through the Al film to form nucleation sites on the sapphire substrate. These sites expand laterally by mass accretion and coalescence to form islands continuous with the underlying substrate. During the final growth sequence, the coalescence of larger island structures is characterized by the presence of twinning zones and defects at the juncture region. Direct observation by TEM/SEM at various stages of annealing confirm that the (structural) regrowth sequence is simialr to that observed during conventional epitaxy of Si on sapphire.[13,14] The presence of twins, stacking faults and dislocation lines is routinely observed in silicon grown by conventional epitaxy on sapphire.[15,16] The regrown silicon layers observed in these experiments exhibit comparable defect densities and distributions of defects within the film.

TABLE 1. ELECTRICAL MEASUREMENTS ON REGROWN SILICON LAYERS

Sample Configuration	$Si/Al/Al_2O_3$	Si/Al/Si (Ref. 10)
Annealing Condition	550^oC, 20 hr.	530^oC, 10 hr.
Sheet Resistivity ($\Omega/\square$)	1260	1100
Hall Mobility ($cm^2/V\text{-}sec$)	30	65
Carrier Concentration (cm^{-3})	3.3×10^{18}	2×10^{18}

3.0 MICROSTRUCTURAL DEFECTS AND LASER-INDUCED REORDERING IN SOS

Epitaxial silicon-on-sapphire (SOS) films used in the electronics industry for fabrication of high-speed, low-power integrated circuits are grown by chemical vapor deposition (CVD) at temperatures close to 1000°C. The (100) Si films are typically 0.5 - 0.6 μm thick and grown on Al_2O_3 substrates of (01$\bar{1}$2) orientation. After cooling down to room temperature, the Si films were found to contain high levels of stacking faults and twins near the sapphire interface[15], as well as compressive stress in the (100) plane[17]. These properties are attributed to: (1) the 100% difference in thermal expansion coefficients, α, between Si and sapphire in the temperature range 25-1000°C ($\alpha_{Si} < \alpha_{Al_2O_3}$), and (2) the 10% mismatch in effective lattice parameters, a, between the two materials ($a_{Si} > a_{Al_2O_3}$); however, the exact structural and chemical configurations of the Al_2O_3 surface during CVD at high temperature are not yet established. Recently, several groups have reported a reduction in defect levels[18] or stress[19,20], in SOS films which had been melted and regrown in the ms time regime by cw Ar laser irradiation. The present study extends some of the earlier investigations and shows that very significant reductions occur in <u>both</u> crystalline defect levels and stress, and that these are interrelated.

3.1 EXPERIMENTAL

The (100) oriented Si epitaxial layers used in this study were grown by chemical vapor deposition on 3 inch diameter sapphire (Al_2O_3) wafers of (00$\bar{1}$2) orientation prepared by Union Carbide Corporation. Thicknesses of the Si

films were in the range, 0.15 μm to 0.40 μm, and the deposition rate was varied between 0.1 μm and 2.4 μm/min. Portions of some wafers were implanted at room temperature (RT) with ^{28}Si or ^{31}P ions, with or without a secondary ^{11}B implant. To avoid excessive sample heating during ion implantation, the beam current density was maintained at a level below 1 $\mu A/cm^2$ during all implants.

Laser irradiations were conducted on a scanning CW-laser annealing system and samples exposed to the laser beam from the Si side, using a multimode line (λ = 0.5 μm). Beam diameters were 100 μm and 140 μm and corresponding scan speeds were 5 and 15 cm/sec, respectively, producing a nominal dwell time of 1-2 msec. Uniformly, irradiated areas were obtained by stepping adjacent scan lines by 20 μm. During laser irradiation, substrates were maintained at RT or 300°C using a resistivity-heated vacuum chuck.

Samples were characterized using optical microscopy, scanning electron microscopy (SEM), MeV $^4He^+$ Rutherford backscattering (RBS), channeling, and transmission electron microscopy/diffraction (TEM/TED).

3.2 RESULTS

Changes in surface morphology, inidicative of melting and resolidification, occured when the laser power/beam diameter ratio, P/ϕ, exceeded a threshold value of, $(P/\phi)_m$ = (4-5) x 10^2 W/cm. At levels of P/ϕ within a window, $(P/\phi)_m < P/\phi \leq 1.20\ (P/\phi)_m$, the laser annealed areas were relatively uniform with minimal or no traces of scan lines. At P/ϕ levels $>1.20\ (P/\phi)_m$, apparent damage or delamination was

observed. The surface uniformity could be improved by additional line scans, although no significant differences could be detected in the channeling spectra for up to 4 repeated line scans. The TEM data also showed no significant alterations or additional improvements in structure after repeated line scans, in agreement with the results from channeling measurements. Areas which had been implanted with Si ions at RT to form a buried amorphous layer were visibly less uniform after laser irradiation than the adjacent control (unimplanted) regions. This is possibly attributed to the higher absorption of the laser light and the lower thermal conductivity of the implanted (amorphous) region. Both channeling measurements and TEM analysis showed no dramatic differences between the implanted and unimplanted regions after laser irradiation. It is interesting to note that the color of the laser irradiated regions (in reflected light) was light yellow, whereas unirradiated regions were darker yellow and implanted (no laser irradiation) areas were dark brown or black.

Rutherford backscattering, channeling energy spectra and detailed angular scans were obtained using a (1-2 mm^2) 1.5 MeV $^4He^+$ beam. The laser annealed SOS structures exhibited a dramatic imrpovement in crystal quality of the epitaxial Si films and the results showed that the films were superior to SOS films of the same thickeness grown or processed by any other technique. As shown in Table 2 and Figs. 3-5, both the surface channeling yield, X_0, and the average dechanneling rate, d_X/dz, were considerably lower than in the starting CVD material, although still above the values obtained for a bulk Si crystal of (100) orientation. In addition, the measured full width at half minimum, $X_{1/2}$, of the angular scans measured for a zone, 500Å below the Si surface was the same in the laser annealed films and (100) bulk silicon (1.1 $\pm$ 0.1°). In comparison,

Thickness (μm) of SOS Film		As Deposited		Laser Annealed		Bulk Si <100>	
		χ_o	$d\chi/dz$ (μm^{-1})	χ_o	$d\chi/dz$ (μm^{-1})	χ_o	$d\chi/dz$ (μm^{-1})
0.37		0.13	1.3	0.063	0.2		0.05
0.20	CVD	0.42	1.5	0.16	0.35	0.04	0.04
	(P+B) Implanted	0.77	-				
0.17		0.26	2.1	0.17	0.3		0.04

TABLE 2. SILICON SURFACE CHANNELING YIELD, χ_o, AND AVERAGE DECHANNELING RATE, $d\chi/dz$, FOR 1.5 MeV $^4He^+$ IONS INCIDENT ON (100) SOS FILMS, BEFORE AND AFTER CW Ar LASER ANNEALING IN THE LIQUID PHASE MODE FOR 1 ms. χ_o IS MEASURED JUST BELOW THE SURFACE PEAK, OR IN THE ABSENCE OF A PEAK, AT THE POSITION OF THE SURFACE SLOPE CHANGE IN THE SPECTRUM. $d\chi/dz$ IS DEFINED AS THE DIFFERENCE BETWEEN THE INTERFACE AND SURFACE YIELDS, DIVIDED BY THE FILM THICKNESS. SINCE THE EXACT VALUES OF $d\chi/dz$ ARE SENSITIVE TO SURFACE CONTAMINATION AND OTHER EXPERIMENTAL CONDITIONS, THEY ARE GIVEN MAINLY TO SHOW THE GENERAL TREND, RATHER THAN AS VIGOROUS QUANTITATIVE DATA.

LIQUID-PHASE, CW Ar LASER ANNEALING OF SOS

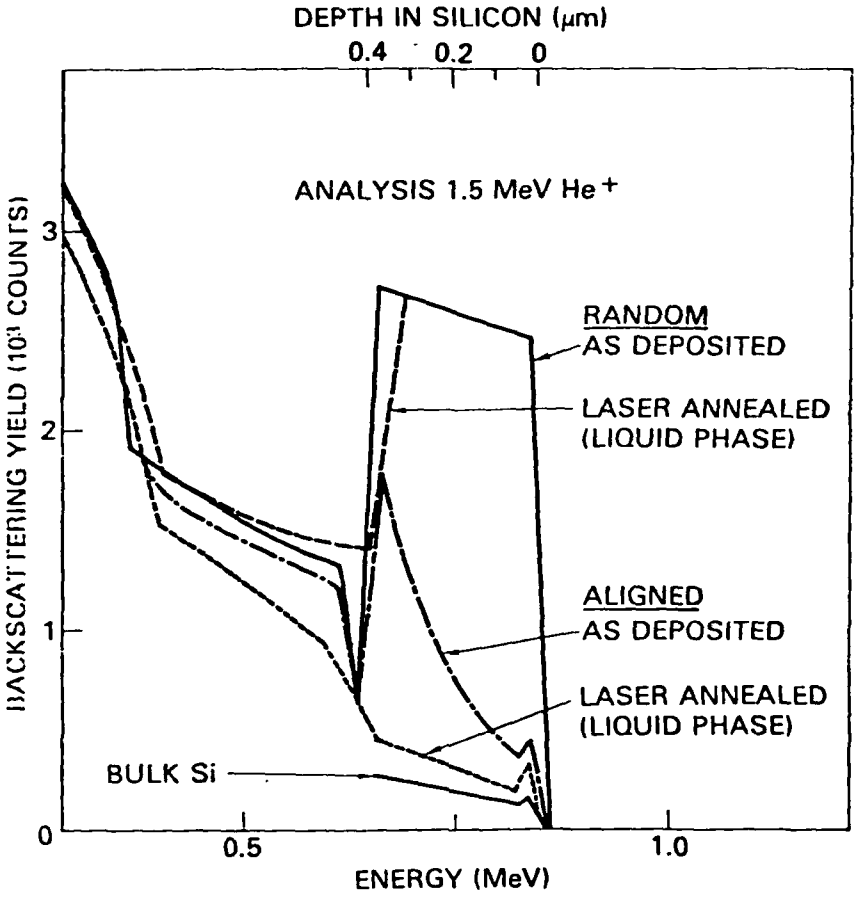

FIGURE 3. ENERGY SPECTRA OF 1.5 MeV $^4He^+$ IONS (1-2 mm^2 SPOT SIZE) BACKSCATTERED AT 170° FROM (100) Si EPITAXIAL FILM OF 0.37μm THICKNESS GROWN ON $(01\bar{1}2)$ Al_2O_3 SUBSTRATE. LASER ANNEAL CONDITIONS: BEAM DIAMETER - 140μm; SCAN VELOCITY-15 cm/sec; SCAN STEP - 20μm; T_s= 300°C; P= 7.5W. ALIGNED SPECTRUM FOR A BULK (100) Si SINGLE CRYSTAL (UNTREATED) IS SHOWN FOR REFERENCE.

LIQUID PHASE, CW Ar LASER ANNEALING OF SOS

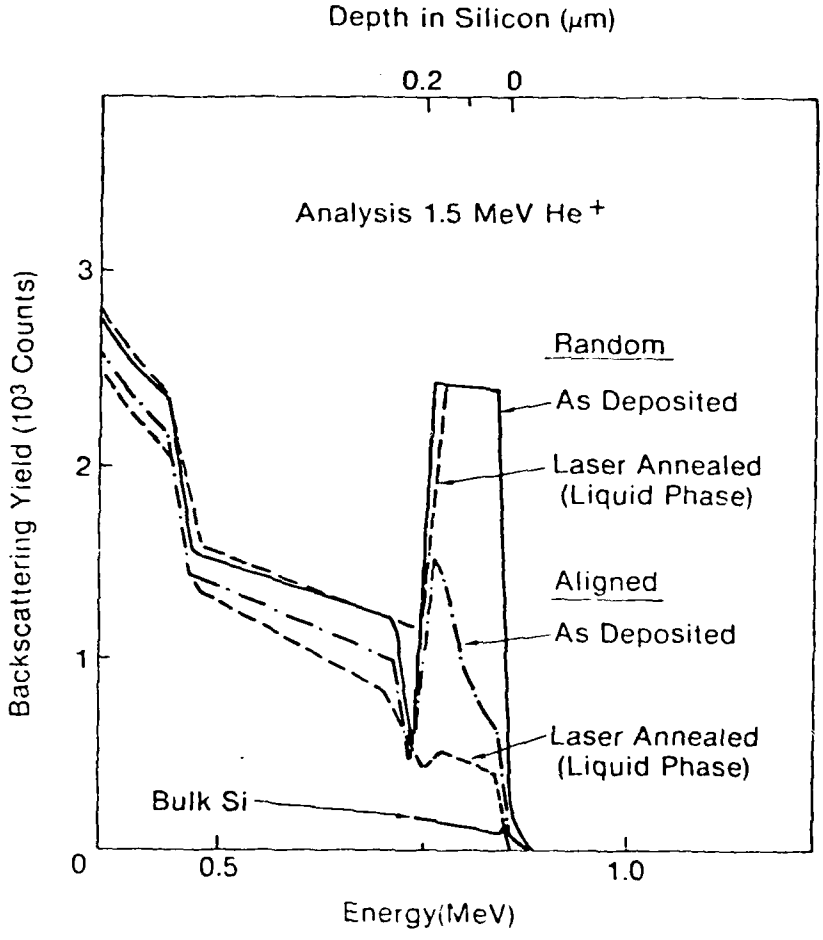

FIGURE 4. ENERGY SPECTRA OF 1.5 MeV $^4He^+$ IONS BACKSCATTERED FROM 0.17 THICK Si LAYER ON SAPPHIRE. LASER ANNEAL CONDITIONS: BEAM DIAMETER - 140μm; SCAN VELOCITY - 15 cm/sec; SCAN STEP - 20μm; T_s= 300°C; P= 7W. ALIGNED SPECTRUM FOR A BULK (100) Si SINGLE CRYSTAL IS SHOWN FOR REFERENCE.

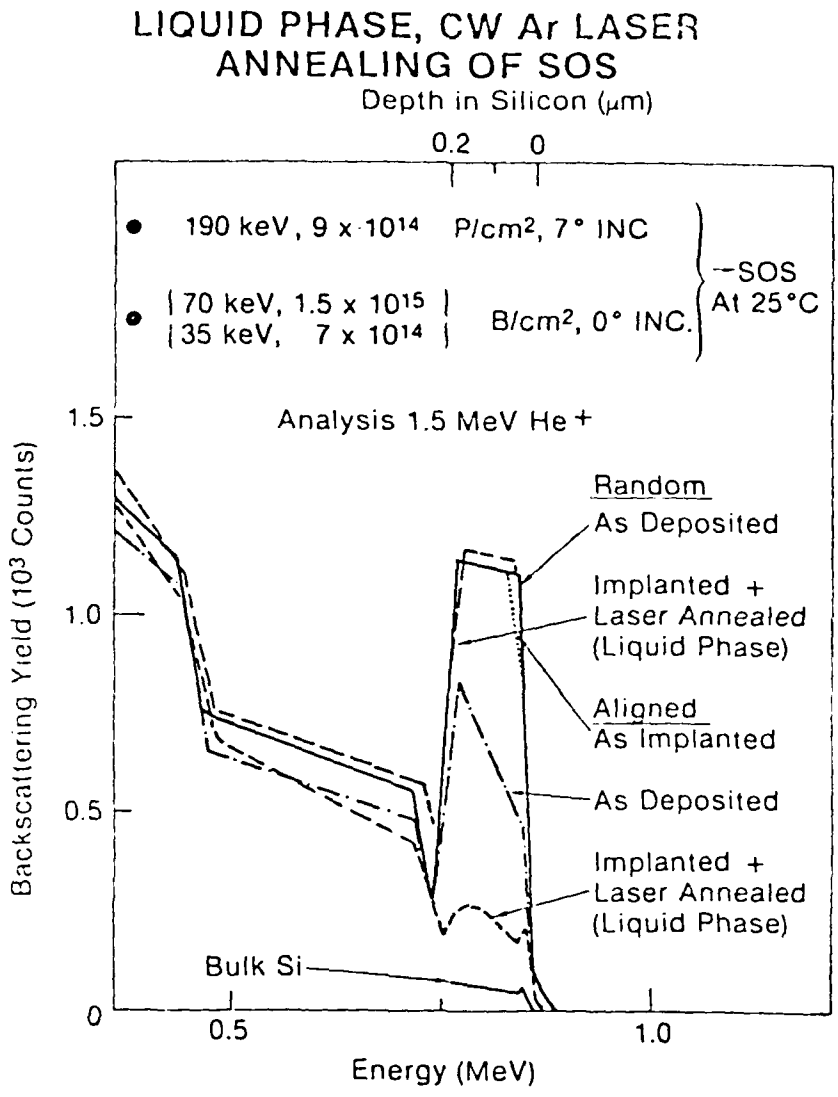

FIGURE 5. ENERGY SPECTRA OF 1.5 MeV $^4He^+$ IONS BACKSCATTERED FROM 0.20μm THICK Si FILM ON SAPPHIRE. AFTER (P + B) IMPLANTATION, THE Si HAD A BURIED AMORPHOUS LAYER EXTENDING TO THE SAPPHIRE INTERFACE, BENEATH A ≈500Å THICK SINGLE-CRYSTAL SURFACE LAYER (DOTTED LINE). THE LASER IRRADIATION WAS DONE UNDER THE FOLLOWING CONDITIONS; BEAM DIAMETER 10μm, SCANNING SPEED 5 cm/s (BIDIRECTIONAL), SCAN STEP 20μm, SUBSTRATE TEMPERATURE 25°C, NOMINAL LASER POWER 5.25W (SLIGHTLY ABOVE THE MELTING THRESHOLD). ALIGNED SPECTRA (NOT SHOWN) MEASURED ON AREAS HAVING (i) ONLY THE P IMPLANT AND LASER IRRADIATION AT 5.25W, or (ii) EITHER P OR (P + B) IMPLANTS AND IRRADIATED AT 5.5W WERE SIMILAR TO THE ALIGNED SPECTRUM SHOWN (DASHED LINE, ALIGNED), WHICH WAS MESSURED ON AN AREA IMPLANTED WITH (P + B) AND LASER IRRADIATED AT 5.25W. THE HIGHER BACKSCATTERING YIELD OF THE RANDOM SPECTRUM MEASURED ON THE IMPLANTED AND LASER IRRADIATED AREA (DASHED LINE, RANDOM) COULD BE DUE TO A 3% ERROR IN CHARGE INTEGRATION.

the values obtained in CVD (no laser irradiation) films were consistently lower than values for bulk (100) Si by a factor of 10-15%. The results then imply that the laser irradiation improves the crystal quality of the Si layers, both at the surface and at depths into the film.

It can be noted that the crystal quality of thick ($t \approx 0.4\,\mu m$) laser irradiated SOS films is improved relative to results obtained for thinner ($t \approx 0.2\,\mu m$) films, as shown in Figs. 3 and 4. Films of the same thickness, but of varying initial crystal quality, produced as a result of varying CVD conditions or post-deposition implantation, exhibited essentially the same high crystal quality after laser exposure (within rhe experimental accuracy of the measurement system), as shown in Figs. 4 and 5. The small differences in shape of the aligned spectra measured on the laser irradiated regions do not alter this conclusion. The observed differences could be caused by: 1) presence of a thin oxide layer at the surface, resulting in the respective absence, or presence of a clearly identifiable surface channeling peak, and 2) the presence of residual damage produced by the implantation on the sapphire side of the interface.

To provide further information on the relative changes in crystal quality in terms of microstructural defects present in as-deposited and laser annealed films, samples were prepared for TEM/TED analysis. Specimens were cut into 3mm x 3mm squares and mechanically abraded from the sapphire side to a total thickness of 20-30μm. Subsequently, samples were subjected to a two-stage Ar-ion milling to produce thin electron transparent regions. Examination of prepared samples was performed using a Siemens 102 electron microscope at an accelerating voltage of 125 kV. Both bright-field and

high resolution dark-field imaging modes were used for all analyses.

Representative bright-field transmission electron micrographs obtained on as-deposited and laser annealed samples are shown in Figs. 6 and 7, for 0.37 μm and 0.17 μm thick Si films, respectively. In the as-deposited films, a large density of stacking faults, twinning zones, and dislocation lines are typically observed, producing large, laterally variable regions of disorder in the films. In all cases, the average density of defects within films was consistently high. In contrast, after laser annealing, a substantial reduction in defect density is observed throughout the film thickness. Regions as large as 25 μm x 25 μm in the laser irradiated regions were found to be defect-free with only an occasional line defect observed in other laser irradiated areas. Consistent with the channeling data, we observed that the thicker films displayed a smaller number of randomly nucleated defects than the thin films. In all cases, it is of significance to note that the presence of prominent twinning observed by TED in the as-deposited films is <u>not</u> detected in the laser irradiated films.

Comparison of both multiply (laser) scanned and laser irradiated ion-implanted films show no significant differences or alterations in cyrstal to the results obtained after a single laser scan of CVD or ion implanted samples. In each case, we observe large regions of defect-free Si and a dramatic change in crystal quality relative to the as-deposited films. Multiple laser scans do not either introduce additional defects or further improve the crystal quality obtained after a single laser (melt-mode) recrystallization consistent with the data obtained from RBS and channeling measurements.

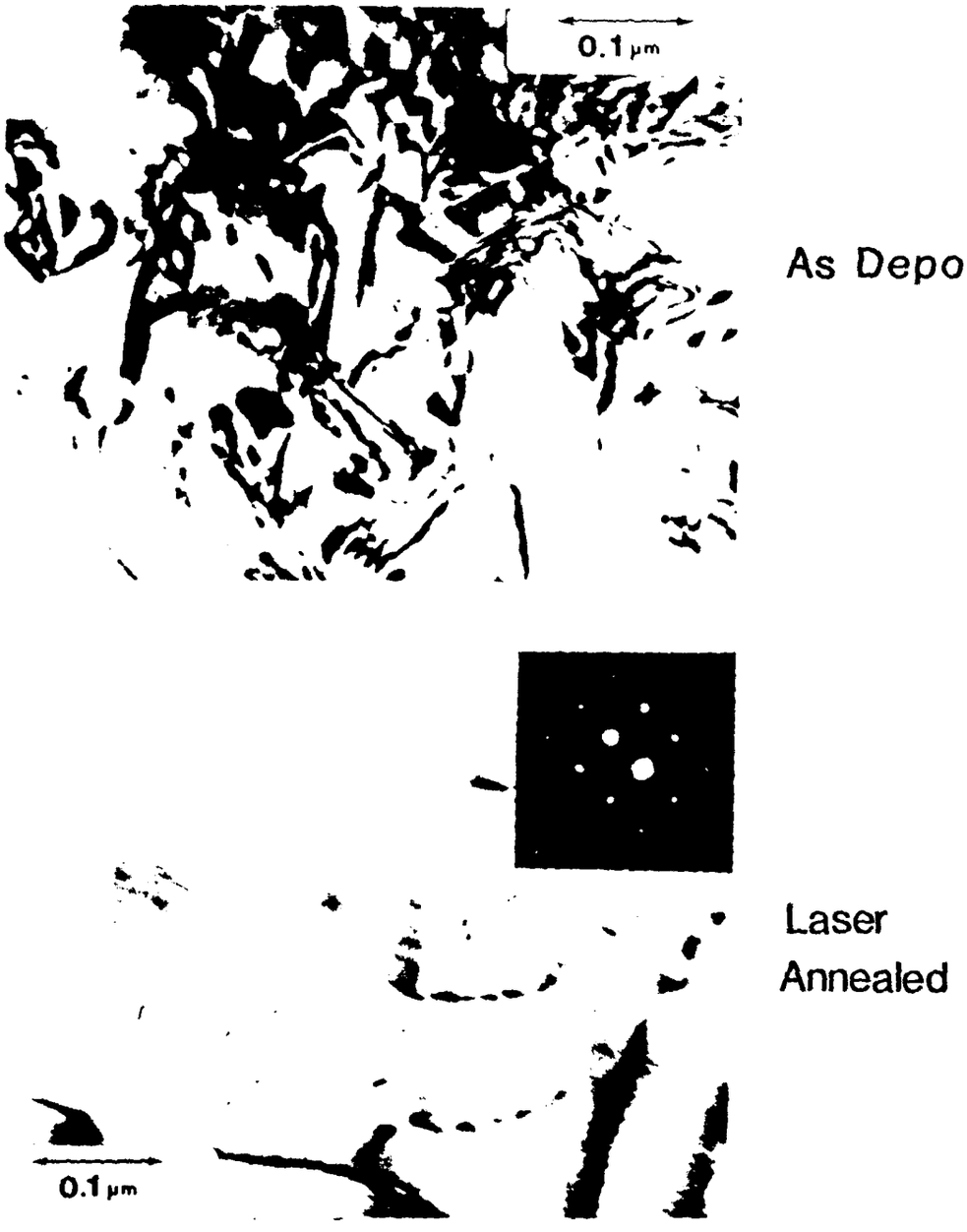

FIGURE 6. PLAN VIEW TRANSMISSION ELECTRON MICROGRAPHS OBTAINED ON AS-DEPOSITED (CVD) AND LASER IRRADIATED SOS FILMS (t_{si} = 0.37 μm) CORRESPONDING TO SAMPLE IN FIG. 3.

FIGURE 7. PLAN VIEW TRANSMISSION ELECTRON MICROGRAPHS OBTAINED ON AS-DEPOSITED (CVD) AND LASER IRRADIATED SOS FILMS (t_{si}= 0.17 μm) CORRESPONDING TO SAMPLE IN FIG. 4.

3.3 DISCUSSION

The results obtained in these experiments indicate that the regrowth mechanism induced by the laser irradiation involves: 1) complete melting of the Si film and 2) subsequent epitaxial regrowth starting at the Si-Al_2O_3 interface. From the data obtained, epitaxial regrowth initiation from the surface of the Si film is neither warranted nor expected. The surface morphology of the films can possibly be further improved by the use of a thin transparent encapsulating layer deposited on top of the Si layer and by increasing the laser beam aspect ratio.

4.0 SEEDED AND LIMITED SEEDED REGROWTH OF Si OVER SiO_2 BY CW-LASER ANNEALING

The recrystallization of amorphous or fine-grained polycrystalline Si layers over (amorphous) dielectric layers to produce oriented single crystal layers subsequent to laser irradiation has received considerable attention over the past two years. In an earlier publication[21] it was shown that patterned polycrystalline Si islands of ≈ 0.5 μm thickness on Si_3N_4 layers could be recrystallized to produce relatively defect-free crystals of (100) orientation after CW-scanning laser annealing. In later papers, Geis et al[22,23] suggested that similar laser induced regrowth could be attained if extremely well defined channels (1000Å depth) were introduced into the dielectric layer underlying the polycrystalline region. However, a recent investigation[24] showed that the laser recrystallized layer over the finely "grooved" dielectric was not composed of a single crystal sheet, but rather a large number of crystallites of varying orientation with respect to the grating. Using a microscopically grooved (spatial period of 1-4 μm) SiO_2 layer, regrowth of fine grained polycrystalline Si films was shown to occur, producing large crystallites in a textured (100) film when laser or strip-heater annealing was employed.

Recently, Tamura et al[25] proposed an alternative approach in which poly-Si films deposited on Si substrates with SiO_2 stripe patterns were annealed with a Q-switched ruby laser to produce apparent lateral growth or "bridging epitaxy" from the Si (substrate) windows onto the adjacent SiO_2 stripe. To test this hypothesis and to determine, if indeed, seeding from the single crystal is observed, or more importantly, whether crystallization can occur over both the

substrate and SiO_2 with limited dependence on seeding from the substrate, a series of laser induced recrystallization experiments were conducted. A similar configuration of oxide bars on single crystal (100) Si with thin polycrystalline Si layers deposited over the oxide and the Si substrate was employed.

4.1 Experimental

Using an Ar-scanning CW-laser system,[26] scan directions and laser powers were varied in separate experiments, and the laser induced reordering of films investigated with bright and dark field transmission electron microscopy (TEM).

Silicon wafers used in this study were p-type (10-20 Ω-cm) of (100) orientation. A 1000Å thick SiO_2 layer was formed on the surfaces of wafers using a 1000°C pyrogenic-steam oxidation process. The oxide was subsequently etched to produce a pattern of 3 μm wide SiO_2 stripes parallel to a (001) direction and separated by 3 μm open channel substrate regions. Using an LPCVD system, a 2000Å thick polycrystalline Si film was then deposited at 620°C over the entire surface. The resulting structure is shown graphically in Fig. 8.

Specimens for TEM or Auger electron spectroscopy analyses were prepared from control or laser annealed samples in the form of 3mm x 3mm squares. A two-stage jet thinning process was used to prepare thin areas with the underlying oxide stripes removed for TEM examination.

Laser annealing was done at a substrate temperature of 375°C using a beam diameter of 45 μm and a scan speed of 10

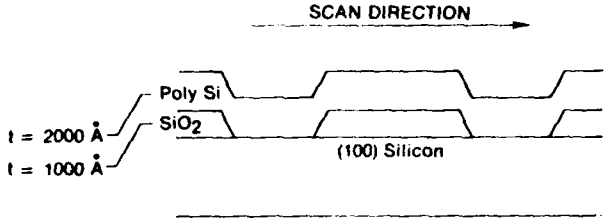

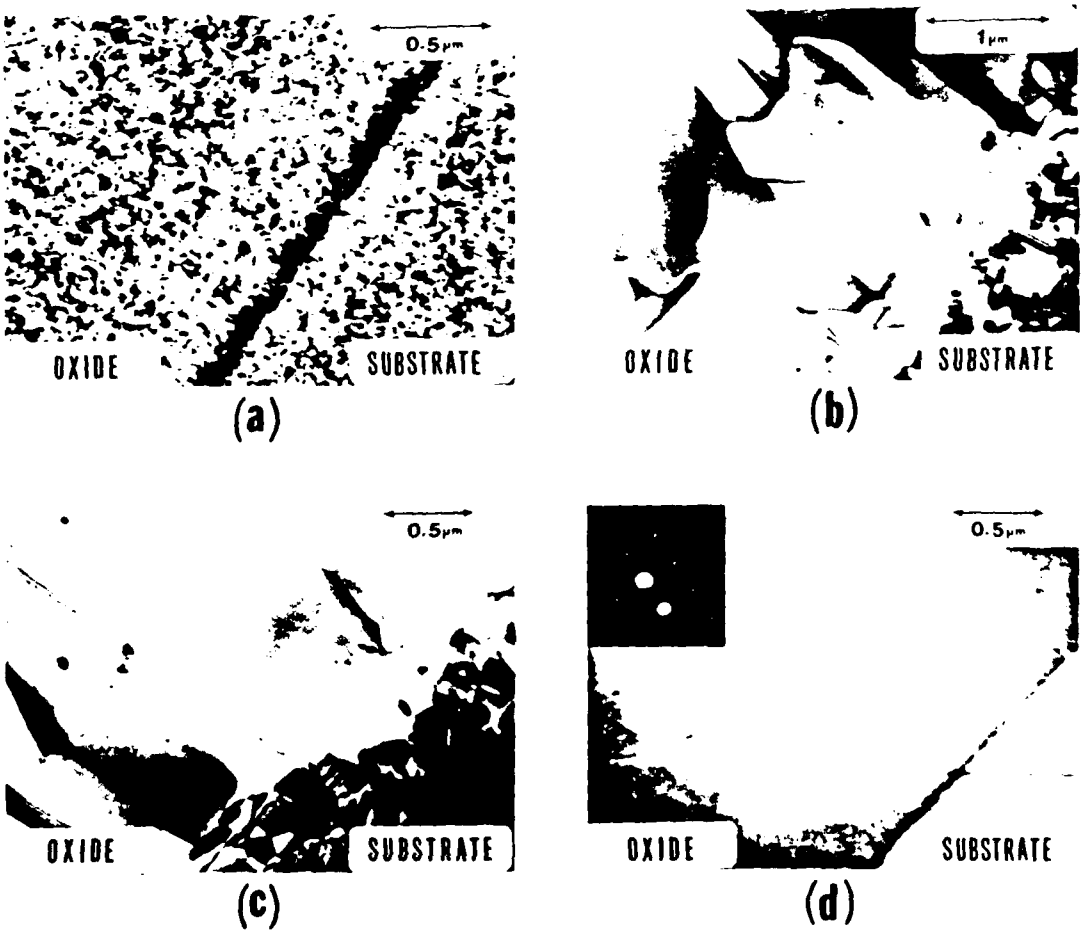

FIGURE 8. CROSS-SECTIONAL SCHEMATIC OF TEST STRUCTURES AND BRIGHT-FIELD TRANSMISSION ELECTRON MICROGRAPH OF CONTROL AND LASER ANNEALED SILICON LAYERS AT THE OXIDE EDGE ZONE; a) AS-DEPOSITED; b) 7W; c) 8W; d) 10 W. THE SELECTED AREA TRANSMISSION ELECTRON DIFFRACTION PATTERN (INSET IN 1d) SHOWS THAT (100) RECRYSTALLIZATION HAS OCCURRED THROUGHOUT THE LASER SCANNED REGION.

cm/sec. In separate experiments, the laser power was varied between 6 and 14W. At a threshold power of 9W, smooth, texture-free, melted lines were observed on the surface. At laser powers >12W substrate melting and non-uniform poly-Si film delamination occurred, thereby restricting the range of usable powers above the threshold level. Prior heat treatment at 1100°C or thin oxide coatings over the poly-Si films did not substantially alter the recrystallization observed in optical or scanning electron micrographs.

4.2 RESULTS

Fig. 8 shows representative bright field electron micrographs obtained on "as-deposited" and laser scanned silicon layers at the edge of the SiO_2 stripe regions. In this case the laser scan direction was perpendicular to the stripe lines and the laser power level varied on separate samples.

In Fig. 8a) the electron micrograph shows the fine grained structure of the as-deposited poly-Si layer. After laser scanning at 7W, the poly-Si layer on the SiO_2 has melted, producing large columnar crystallites of varying orientation (Fig. 8b)). In contrast, only a slight increase in average grain size can be detected within Si layers over the substrate region. Increasing the laser power to 8W produces an additional increase in the size of columnar grains over the SiO_2, accompanied by small increases in grain size of the poly-Si layer over the substrate (Fig. 8c)). After either 7 or 8W laser scans, we detected evidence of limited mass flow downward from the SiO_2 stripe area onto the fine grained poly-Si layer.

When the laser power is increased to $\geq$9W, melting of the Si layer occurs over both the SiO_2 stripes and single crystal layer of (100) orientation (Fig. 8d)). Optical, SEM and TEM examination show that a smooth single crystal (100) Si sheet is produced of approximate dimensions, 100 μm x 10,000 μm, when consecutive overlapping scans are used. The 100 μm width was chosen to provide a suitable region for examination by TEM. Wider recrystallized regions should be attainable when the number of overlapping scan lines is increased. In the present experiments, we did not detect the presence of twinned regions, extended mosaic structure, stacking faults or defective SiO_2 edge recrystallization zones under the experimental conditions utilized. Thickness contours were continuous across the recrystallized region, indicating the absence of growth discontinuities or cracks in the regrown layer. The amount of scan line overlap was found to be an extremely important factor. If insufficient line overlap was used, edge zones containing dislocation lines were observed within the overlap regions. For overlap factors $\geq$40%, residual defect structure was not detected.

In this study we observed that critical edge definition on the SiO_2 stripe[22,27] is not a particularly crucial factor in these experiments and relatively small variations do not effect recrystallization. In like manner, we found that an SiO_2 layer deposited on top of the polysilicon layer is not required for production of smooth single crystal sheets. However, a thin (<100Å) SiO_2 layer is normally produced on top of the recrystallized Si during laser anneals in air, as confirmed by Auger electron spectroscopy profiling.

In additional experiments, we determined that relatively defect-free single crystal sheets of (100) orientation containing no mosaic structure or internal crystallites can be produced, independent of laser scan direction. However, the data do not conclusively establish that bridging epitaxy or seeding from the single crystal substrate has occurred, or to what degree seeding is important for growth over the SiO_2. In previous experiments,[21] we showed that defect-free single crystal Si bars of (100) orientation on SiO_2 can be formed after scanning laser annealing. At laser powers below the threshold power level for single crystal formation, large columnar crystallites were formed, producing an array similar to that observed over the SiO_2 layers in Figs. 8b) and c). Since single crystal regrowth of Si over SiO_2 can occur independent of seeding in patterned arrays and since there is a 2W differential for melting of the Si layer over the single crystal window and SiO_2 layer, the thermal boundary conditions at the SiO_2 edge may be sufficiently stringent with CW laser annealing to limit or place severe restrictions on the conditions needed to assure lateral growth of Si over the SiO_2 from the substrate region.

To further investigate this possibility, we performed another set of experiments to effectively isolate edge growth and vertical regrowth over the SiO_2 stripe. Samples were scanned in a direction parallel to the oxide stripes, using a laser power of 12W and parameters identical to those used in the previous experiments. In a series of tests we attempted to place the beam scan line with respect to the oxide strip direction to define a region along the edge of the beam profile where the equivalent laser power over the oxide strip would be sufficient to melt the Si layer, but owing to the approximate Gaussian nature of the beam profile, would only

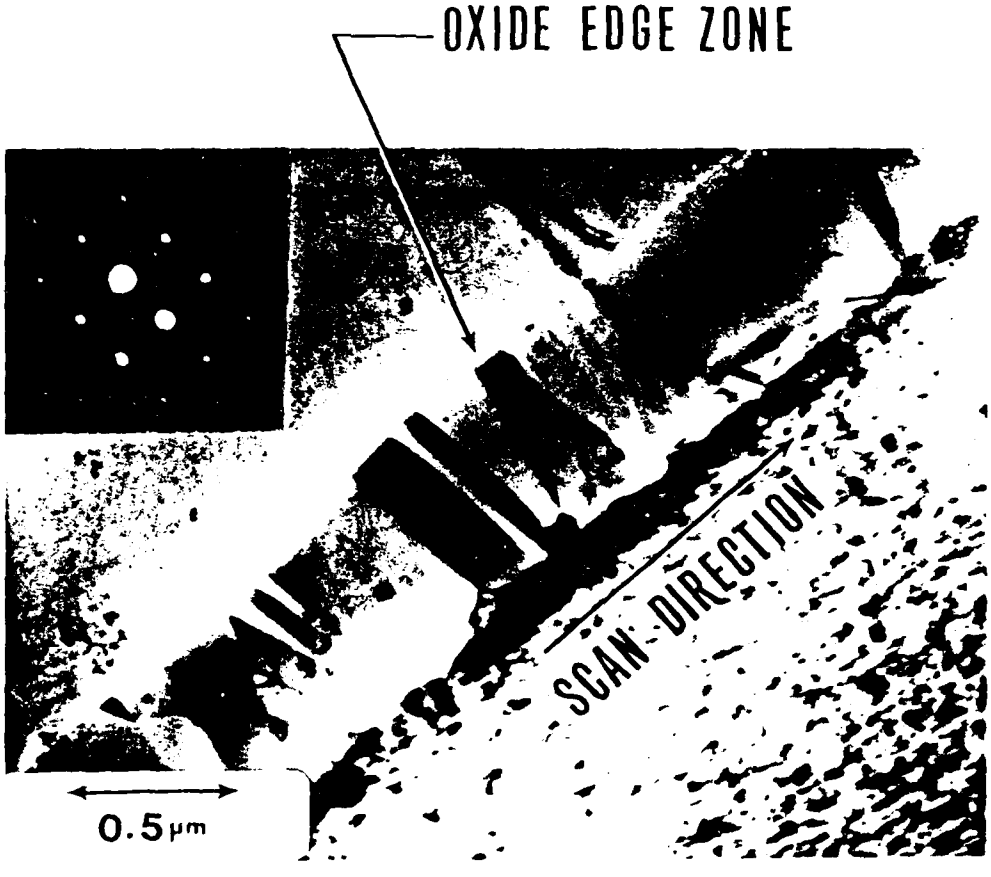

FIGURE 9. BRIGHT-FIELD TRANSMISSION ELECTRON MICROGRAPH OF DISTINCT SILICON REGROWTH REGIONS NEAR THE OXIDE-SILICON EDGE REGION. INSET SHOWS TRANSMISSION ELECTRON DIFFRACTION PATTERN OBTAINED FROM LAYER OVER SiO_2 BAR, INDICATING SINGLE CRYSTAL (100) Si.

the recrystallization. In Fig. 2 we show a transmission electron micrograph of such a region. Within the layer atop the single crystal substrate, melting has occured within a zone adjacent to the oxide edge, extending to a maximum width of 0.75 μm. Crystallites are formed on the Si substrate and extend up the edge of the oxide bar. Over the oxide stripe to the left, melting and recrystallization have occurred, producing a continuous single crystal area of (100) orientation. We observed no distinct correlation between the recrystallization at the peripheral regions of the oxide and single crystal growth over the oxide bar. If seeding from the substrate window were the dominant mechanism, we would anticipate a mosaic or large grained structure over the SiO_2, seeded from the crystallites shown at the edge region. Since only single crystal lines are observed on top of the SiO_2, we can infer that single crystal growth can occur, independent of any seeding or lateral growth from the substrate window.

4.3 DISCUSSION

Under the experimental conditions used in this study we can conclude that texturing, spreading epitaxy or vertical seeding from the single crystal substrate is not necessary or a required factor for growth of the Si layer over the SiO_2 stripe. It has been suggested by Geis et al[24] that stress induced in the silicon film as a result of thermal expansion differences between Si and SiO_2 may be responsible for development of (100) crystallization. Stresses induced in the underlying oxide may account for the observed development of selective crystallization over the SiO_2 stripes with relaxed requirements for lateral seeding.

At the high scan rates (10 cm/sec) used in these experiments, a thick oxide is not formed on the Si films during laser anneals in air, thereby emphasizing the possible importance of stresses in the underlying oxide. Since single crystal growth can occur over both the substrate and oxide bars in separate regrowth modes, the influence of thermal boundary conditions at the oxide edge will also be an extremely important factor in defining smooth edge juncture growth with an apparent absence of defects. Experiments are continuing to further evaluate mechanisms responsible for the observed regrowth and will be reported in a later publication.

5.0 LASER ASSISTED DIFFUSION AND ACTIVATION OF TIN FROM AN SnO_2/SiO_2 SOURCE

The diffusion of impurities into a semiconductor substrate from a deposited thin film source has been investigated for a number of years. Recently, the use of a SnO_2/SiO_2 source to diffuse Sn impurities into GaAs substrates has been introduced [28-30] and found to have propoerties of interest for GaAs technology. In cooperative experiments with Stanford University, we have investigated the metallurgical modifications induced after thermla and scanning laser annealing of spin-on SnO_2/SiO_2 layers on GaAs substrates.

5.1 Experimental

Semi-insulating, Cr-doped GaAs substrates of (100) orientation were coated with a double "source cap" layer consisting of a 0.3 μm spin-on SnO_2/SiO_2 film covered by a 0.5 μm CVD-SiO_2 film. To prevent delamination of the double layer source-cap during laser irradiation, a slow thermal ramp was carried out in a flowing N_2 environment. Typical thermal pre-treatment for optimum results consists of a ramp from room temperature to 900°C in 15 minutes. This step breaks down the barrier introduced by a native oxide layer, produces initial intermixing and allows the diffusion process to proceed.

Following thermal ramping, samples were subjected to scanning CW-Ar laser annealing using a beam spot diameter of 50 μm, a scan velocity of 12 cm/sec and a scan step spacing of 15 μm between lines. To reduce thermal stress, the substrate was maintained at a temperature of 350°C during laser irradiation. Using calculations and curves of laser induced temperature in GaAs, the maximum surface temperature was obtained for each laser power level used in the experiments.

5.2 Results

The diffusion of tin was first studied in a regime where the laser power was kept below the level required to melt the substrate. The laser power for this condition was determined by observing the laser power required to just produce visible thermal etching and then reducing the settings by 5%. A power level of P = 0.61W, leading to a maximum induced temperature of about 800°C, was obtained. A series of 1, 3 and 5 scan frames were performed with the double layer "source-cap" remaining on the substrate. A Van der Pauw technique was used to characterize the resulting sheet resistivity, Hall mobility and sheet carrier concentration. The results are summarized in Table 3. The increase of the sheet carrier concentration from 2.44 to 3.01 x 10^{13} cm^{-2}, accompanied by a decrease of sheet resistivity with a larger number of scans, illustrates the diffusion process.

SIMS analysis was performed on a sample thermally ramped only and on a sample scanned 5 times after the ramping. The profiles show ans increase in Sn concentration and an in-diffusion of about 150 Å. To investigate the contribution of the irradiation to the diffusion form the source-cap, compared to the activation of the impurity sitting in the substrate after the ramp, the source was removed before the laser scans. The reflectivity of the bare substrate (after the thermal ramp) was measured and the incident laser power adjusted to reach the same maximum temperature (800°C) as before. The wafer was scanned five times and the sheet electrical measurements presented in Table 3 were carried out. The results, when compared with those obtained with the "source-cap" on, suggest that the total increase in active impurities due to laser irradiation is 77% from the source and 23% from the activation of Sn introduced during the ramp.

TABLE 3

SHEET ELECTRICAL MEASUREMENT OF THE Sn DIFFUSED LAYER INDUCED BY REPETITIVE LASER SCANS

	$\rho(\Omega/\square)$	μ_H (cm^2/V.sec)	N_s (cm^{-2})
Thermal Ramp to 900°C in 15 Min.	122	2098	2.44×10^{13}
1 Scan with "Source Cap"	118	2017	2.63×10^{13}
3 Scans with "Source Cap"	117	1838	2.91×10^{13}
5 Scans with "Source Cap"	107	1940	3.01×10^{13}
5 Scans with NO "Source Cap"	118	2057	2.57×10^{13}

The action of the laser is found to be more significant if the sample is left "at temperature" for a short time after the ramp. For this reason, the above experiment was repeated after thermally ramping the substrate and its source to 900°C and leaving it for 5 minutes longer at 900°C. A series of 5 scans inducing a maximum temperature of about 800°C was then performed. A differential van der Pauw technique was used to profile these samples. Figure 6 shows the results obtained before and after irradiation. A net increase in carrier concentration to a value of about 8×10^{13} is observed after the scans. The total Sn profile was also obtained using a Rutherford backscattering system. A 2.2 MeV incident helium beam incident on the GaAs substrate was used after removal of the source. A sample having received a thermal treatment only, another one receiving additional laser scans leading to $T_{max} \simeq 800°C$, and a third one scanned at higher laser power leading to $T_{max} \simeq 850°C$, were analyzed. The Sn profile is characterized by a large peak concentration at the surface which increased after laser scan, probably showing Sn diffusing from the source.

Both the R.B.S. profiles and those obtained using SIMS analysis show an anomalously high concentration of Sn close to the surface. This suggests that a chemical reaction takes place in addition to the diffusion process. To study this possibility, a sample ramped to 900°C and a sample ramped and scanned 5 times at a power inducing a temperature of 800°C, were prepared for T.E.M. and diffraction analysis using conventional jet thinning techniques. Bright-field (Fig. 11) and dark-field transmission electron micrographs indicated precipitation after thermal ramp and after laser processing. Selected area electron diffraction patterns revealed that the precipitates were composed of a tin arsenic compound: Sn_3As_2. Additionally, an amorphous β-Ga_2O_3 was detected in

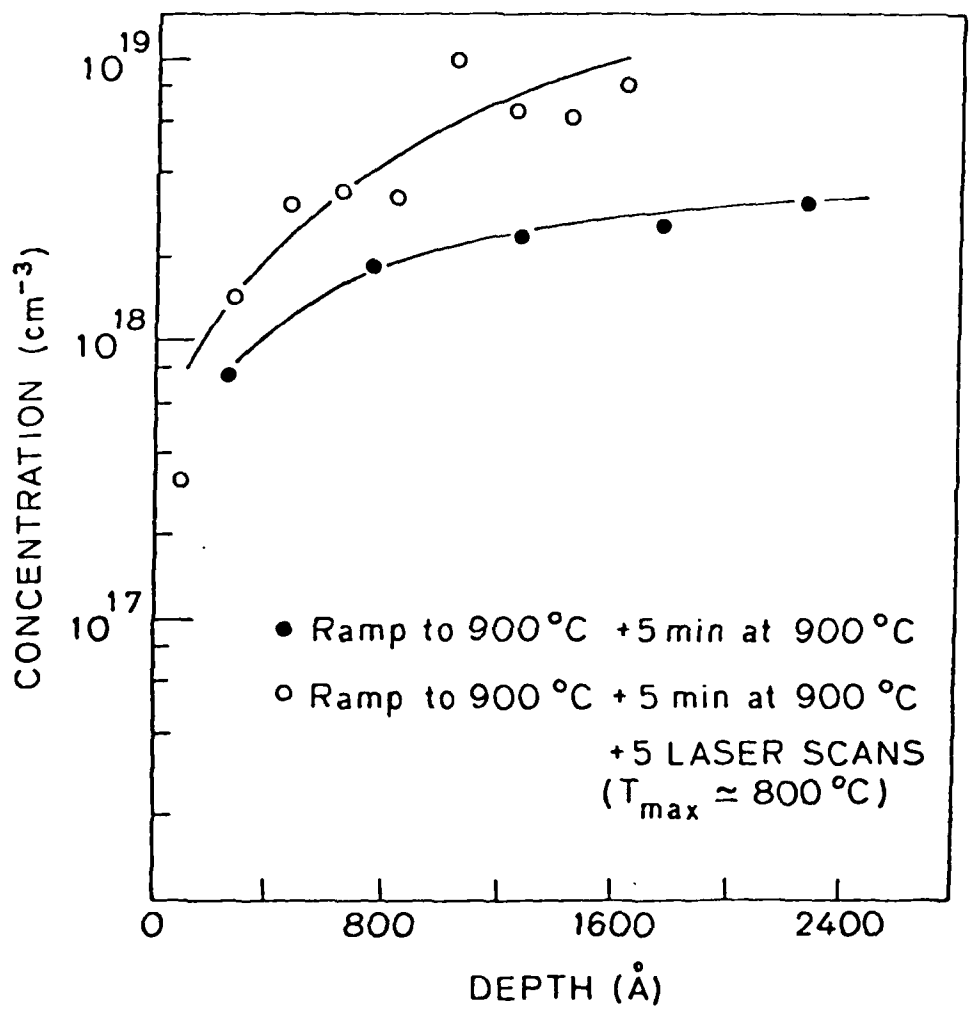

FIGURE 10. ELECTRICAL PROFILES FOR Sn OBTAINED USING A DIFFERENTIAL VAN DER PAUW TECHNIQUE.

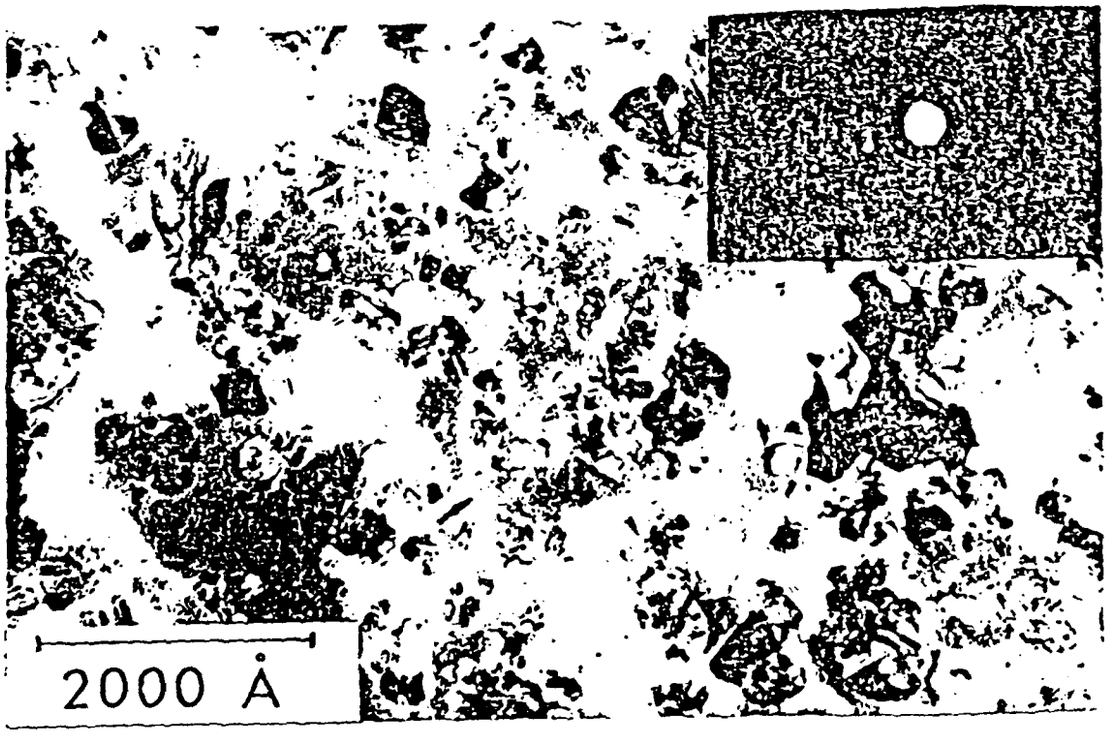

FIGURE 11. BRIGHT-FIELD TRANSMISSION ELECTRON MICROGRAPH SHOWING FORMATION OF As_2Sn_3 PLOTS. IN THE UPPER RIGHT HAND CORNER ARE THE RINGS ASSOCIATED WITH βGa_2O_3 AND As_2Sn_3. THE d VALUES WERE MEASURED AND CHECKED TO BE CONSISTENT WITH ABOVE COMPOUNDS.

the samples. After laser irradiation, we observed an increase of the amount of surface coverage by β-Ga_2O_3 crystallites. In all cases, the surface oxide film appeared as a laterally discontinuous film.

5.3 Discussion

From the results obtained it has been shown that CW-scanning laser annealing can assist in the diffusion and activation of Sn in GaAs. The observed increase in Sn concentration and the subsequent substantial increase in Sn_3As_2 precipitates after thermal ramping and laser annealing show that a simple "doping" model cannot alone explain the effective formation of the n^+ layer and that the alloy formation is correlated with the observed activity. In either case, the technique described appears attractive for GaAs contact technology.

REFERENCES

1. J.O McCaldin and H. Sankur, Appl. Phys. Lett. 19, 524 (1971).

2. H. Sankur, J.O. McCaldin and J. Devaney, Appl. Phys. Lett. 22, 64 (1973).

3. J. Basterfield, J.M. Shannon and A. Gill, Solid State Electron. 18, 290 (1975).

4. J.S. Best and J.O. McCaldin, J. Appl. Phys. 46, 4071 (1975).

5. T.J. Magee and J. Peng, J. Appl. Phys. 49, 4284 (1978).

6. K. Nakamura, M.A. Nicolet, J.W. Mayer, R. J. Blattner and C.A. Evans, Jr.,J. Appl. Phys. 46, 4678 (1975).

7. K. Nakamura, J.O. Olowolafe, S.S. Lau, M.A. Nicolet and J.W. Mayer, J. Appl. Phys. 47, 1278 (1976).

8. K. Nakamura, S.S. Lau, M. A. Nicolet and J.W. Mayer, Appl. Phys. Lett.28, 277 (1976).

9. R.L. Boatright and J.O McCaldin, J. Appl. Phys. 47, 2260 (1976).

10. G. Majni and G. Ottoviani, Appl. Phys. Lett. 31, 125 (1977).

11. G. Majni and G. Ottoviani, J. Cryst. Growth 45, 132 (1978).

12. F.A. Trumbore, Bell Syst. Tech. J. 39, 205 (1960).

13. B.A. Joyce, R.J. Bennett, R.W. Bickness and P.J. Etter, Trans. Met. Soc. AIME 233, 556 (1965).

14. G.W. Cullen and F.C. Dougherty, J. Cryst. Growth 17, 230 (1972).

15. W.E. Ham, M.S. Abrahams, C.J. Buiocchi and J. Blanc, J. Electrochem. Soc.124, 634 (1977).

16. S.S. Lau, S. Matteson, J.W. Mayer, P. Revesz, J. Gyulai, J. Roth, T.W. Sigmon and T. Cass, Appl. Phys. Lett. 34, 76 (1979).

17. Y. Nishi and H. Hara, Japn. J. Appl. Phys. 17, 27 (1978).

18. I. Golecki, G. Kinoshita, A. Gat and B.M. Paine, Appl. Phys. Lett. 37, 919 (1980 amd 38, 648 (1981).

19. G. A. Sai-Halasz, F.Fang, T.O. Sedgwick and A. Segmuler, Appl. Phys. Lett. 36, 419 (1980).

20. M. Yamada, S. Hara, K. Yamamoto and K. Abe, Japan J. Appl. Phys.19, L261 (1980).

21. J.F. Gibbons, K. F. Lee, T.J. Magee, J. Peng and R. Ormond, Appl. Phys. Lett. 34, 831 (1979).

22. M.W. Geis, D.C. Flanders and H.I. Smith, Appl. Phys. Lett. 35, 71 (1979).

23. M.W. Geis, D.C. Flanders, D.A. Antoniadis amd H.I. Smith, J. Vac. Sci. Technol.16, 1640 (1979).

24. M.W. Geis, D.A. Antoniadis, D.J. Silversmith, R.W. Mountain and H.I. Smith, Appl. Phys. Lett. 37, 454 (1980).

25. M. Tamura, H. Tamura and T. Tokuyama, Japanese J. Appl. Phys. 19 L-23 (1980).

26. L.J. Palkuti, J. Peng, C. Welles and T.C. Teng, Proceedings of the 30th Electronics Components Conference, IEEE Cat. No. 80 Ch 1568-5, 37 (1980).

27. D.C. Flanders, MIT Lincoln Lab Tech. Rpt. 533 (1978).

28. I. Arnold, H. Dambkes and K. Heimy, Digest of Tech. Papers, 11th Int'l. Conf. on Solid State Devices, Tokyo, Japan (1979).

29. J.F. Gibbons, A. Leitoila, Y.I. Nissim and F.C. Wu, Proc. 1979 Materials Research Soc., Symposium on Laser and Electron Beam Processing of Materials (unpublished).

30. Y.I.Nissim, J.F. Gibbons, C.A. Evans,Jr., V.R. Deline and J.C. Norberg, Appl. Phys. Lett. 37, 90 (1980).

APPENDIX I

Publications

1. T.J. Magee and J. Peng, J. Appl. Phys. 51, 3973 (1980).

2. T. J. Magee, L.J. Palkuti, R. Ormond, C. Leung and S. Graham, Appl. Phys. Lett. 38, 248 (1981).

3. Y.I. Nissim, J.F. Gibbons, T.J. Magee and R. Ormond, J. Appl. Phys. 51 (1981).

4. I. Golecki, H.L. Glass, G. Kinoshita and T.J. Magee, Proc. Int'l. Conf. on Surface Analysis, (1981), Dayton, Ohio (Plenum Press).

APPENDIX II

Technical Papers Presented

1. T. J. Magee: (Invited Paper) "Microstructural Defects in Laser Annealed SOI", Electronic Materials Conference, Santa Barbara, CA (June, 1981).

END

DATE
FILMED

04-82

DTIC